

Learning-to-Cache: Accelerating Diffusion Transformer via Layer Caching

Xinyin Ma¹ Gongfan Fang¹ Michael Bi Mi² Xinchao Wang^{1*}

National University of Singapore¹ Huawei Technologies Ltd.²

maxinyin@u.nus.edu, xinchao@nus.edu.sg



Figure 1: (a) Generate 512×512 images using DiT-XL/2, sampled by DDIM with 50 NFEs. (b) Generate 256×256 images using U-ViT-H/2, sampled by DPM-Solver-2 with 50 NFEs.

Abstract

Diffusion Transformers have recently demonstrated unprecedented generative capabilities for various tasks. The encouraging results, however, come with the cost of slow inference, since each denoising step requires inference on a transformer model with a large scale of parameters. In this study, we make an interesting and somehow surprising observation: the computation of a large proportion of layers in the diffusion transformer, through introducing a caching mechanism, can be readily removed even without updating the model parameters. In the case of U-ViT-H/2, for example, we may remove up to 93.68% of the computation in the cache steps (46.84% for all steps), with less than 0.01 drop in FID. To achieve this, we introduce a novel scheme, named **Learning-to-Cache** (L2C), that learns to conduct caching in a dynamic manner for diffusion transformers. Specifically, by leveraging the identical structure of layers in transformers and the sequential nature of diffusion, we explore redundant computations between timesteps by treating each layer as the fundamental unit for caching. To address the challenge of the exponential search space in deep models for identifying layers to cache and remove, we propose a novel differentiable optimization objective. An input-invariant yet timestep-variant router is then optimized, which can finally produce a static computation graph. Experimental results show that L2C largely outperforms samplers such as DDIM and DPM-Solver, alongside prior cache-based methods at the same inference speed.

*Corresponding author

1 Introduction

In recent years, diffusion models [60, 59, 19] have achieved remarkable performance as powerful generative models for image generation [49, 10]. Among the various backbone designs for diffusion models, transformers [62] have emerged as a strong contender, showing its exceptional capabilities not only in synthesizing high-fidelity images [46, 3] but also in video generation [38, 7, 4], text-to-speech synthesis [33, 21, 61] and 3D generation [41, 5]. The diffusion transformer, while benefiting greatly from the great property of scalability of the transformer architecture, however, also brings about significant challenges in efficiency, including high deployment costs and slow inference speed.

Since the cost of sampling increases proportionally with the number of timesteps and the model size per timestep, naturally, current methods for increasing the sampling efficiency entail two branches: reducing the sampling steps [57, 19, 34, 2] or reducing the inference cost per step [16, 67]. The methods to reduce the number of timesteps include distilling the trajectory into fewer steps [52, 58, 39], discretizing the reverse-time SDE or the probability flow ODE [57, 73, 37]. Methods in another branch are mainly about compressing the model size [25, 30] or using a low-precision data format [18, 53]. A new method in the dynamic inference of diffusion is a special cache mechanism in the denoising process [40, 64]. These methods leverage the high similarity between the two steps and the special property of U-Net to cache some of the computations, which would be directly used in the next step. Some other dynamic inference methods employ a spectrum of diffusion models and allocate different networks for different steps [65, 44].

Previous approaches, especially those aimed at reducing model size, have predominantly targeted the compression of the U-Net architecture [50]. Our objective is to explore a paradigm for inference acceleration that is more suitable for transformer-based diffusion models. Unlike other architectures, transformers are distinctively composed of several layers with consistent structure. Based on this property, previous compression work on transformers mainly focuses on layer pruning [71] and random layer dropping [14, 48], as optimizing at the layer level tends to achieve higher speedup ratios compared to width pruning [24, 15, 8]. However, for diffusion transformers, we observed that dropping layers without retraining is not feasible. Removing even a few layers significantly degrades image quality (see Section 4.3). This observation highlights that the redundancy among layers at varying depths is not evident in DiT. Therefore, we consider another perspective of redundancy: the redundancy across layers situated at the same depths but occurring at different timesteps.

Motivated by cache-based methods [40, 64, 28], we aim to explore the existence and limitations of layer redundancy between timesteps within the diffusion transformer. A straightforward approach involves an exhaustive search where each layer is either cached or not, resulting in an exponentially growing search space with the depth of the layers. Additionally, heuristic-based layer selection cannot adequately address the mutual dependencies between layers. To overcome these challenges, we designed a framework that makes the problem of layer selection differentiable. Specifically, we interpolate predictions between two adjacent steps. This interpolation spans two extremes: a fast configuration where all layers are cached at the expense of image quality, and a slow configuration where all layers are retained, achieving optimal performance. We then search this interpolation space to identify an optimal caching scheme, optimizing a specialized router. This router is time-dependent but input-invariant, allowing the creation of a static computation graph for inference. We train this router by formulating an optimization problem that does not require updating model parameters, making it both cost-effective and easy to optimize.

Our results indicate that different percentages of layers can be cached in DiT [41] and U-ViT [3]. Notably, for U-ViT-H/2 on ImageNet, approximately 93.68% of layers are cacheable in the cache step, whereas for DiT-XL/2, the cacheable ratio is 47.43%, both with an almost negligible performance loss ($\Delta\text{FID} < 0.01$). By comparison, with the same acceleration ratio, a sampler with fewer steps would compromise image quality. Our method L2C can significantly outperform the fast sampler, as well as previous cache-based methods. Additionally, we observed distinct sparsity patterns for layers between these two models, suggesting significant behavioral variations between different architecture designs for diffusion transformers.

In summary, our contribution is the proposal of a novel acceleration method, learning-to-cache (L2C), specifically for diffusion transformers. We convert the non-differentiable layer selection problem into a differentiable optimization problem by interpolation, facilitating the learning of layer caching. Our results demonstrate that a large proportion of layers in the diffusion trans-

former can be cached without compromising performance. Furthermore, our approach significantly outperforms samplers with fewer steps and other cache-based methods. The code is available at <https://github.com/horseee/learning-to-cache>

2 Related Work

Transformers in Diffusion Models. Diffusion models have demonstrated broad applicability across various domains[13, 4, 69]. Transformer [62] is applied in diffusion models as an alternative to UNet[50]. GenViT[68] integrates the ViT[12] architecture into DDPM. U-ViT [3] employs the long skip connections between shallow and deep layers. DiT [46] shows the scalability of diffusion transformers and is further used as a general architecture for text-to-video generation [4, 38], speech synthesis [33] and 3D generation [5].

Acceleration of Diffusion Models. Generating images by diffusion models requires several rounds of model evaluation which is time-expensive. Some works focus on reducing the number of sampling steps in a training-free manner. DDIM[57] extends the original DDPM to non-Markovian cases. DPM-Solver[36, 37] further approximates the solution of diffusion ODES by the exponential integrators. EDM[23] finds that the Heun’2 2nd order method provides an excellent tradeoff between truncation error and NFE. More works try to solve either SDEs[60, 22, 11] or ODEs[34, 73, 72] in a more accurate and fast way. Other training-based methods [52, 31] distill and half the sampling steps. [58, 39] learns to map any point on the ODE trajectory to its origin. Another line of work reduces the workload per step. The model per step is compressed by reducing the parameter size [16, 6, 71, 63], using reduced precision [29, 18] and re-design the structure of the diffusion model [67, 30, 75, 25, 35]. In addition to static model inference, dynamic model inference has also been extensively explored within diffusion models, which employs different models for inference at varying steps. [32, 45] switch between different sizes of models in a model zoo. [42] designs a time-dependent exit schedule to skip a subset of parameters. Other works focus on denoising diffusion models in parallel[9], either through iterative optimization[54] or image splitting[27]. In addition to inference acceleration, some works also show how to train a diffusion model more efficiently by employing different training paradigm [17, 76] or from the data perspective [47].

Cache in Diffusion Models Cache [55] is used in computer systems to hold temporarily those portions of contents in the main memory which is believed to be used in a short time. Recently, [40, 64, 1] explores the cache mechanism in diffusion models. Based on the observations that the similarities of high-level features [70] is typically very high in consecutive steps, they propose to reuse the feature maps. By utilizing the computation flow of U-Net, [40] reuse the high-level features while updating the low-level features. [64, 28] further discovers the better position in U-Net to be cached. [20] proposes to reuse the attention map. [64, 56, 40] adjust the lifetime for each caching features and [64] further scales and shifts the reused features. [74] finds the cross-attention is redundant in the fidelity-improving stage and can be cached. [66] hashes and caches the images rendered from camera positions and diffusion timesteps to improve the efficiency of 3D generative modeling.

3 Method

3.1 Preliminary

The forward diffusion process starts at the starting point \mathbf{x}_0 , where \mathbf{x}_0 is sampled from the data distribution $q(\mathbf{x}_0)$ to be learned. \mathbf{x}_0 is degenerated with gradually added Gaussian noise, with:

$$\mathbf{x}_t \sim q(\mathbf{x}_t | \mathbf{x}_0) = \mathcal{N}(\mathbf{x}_t; \alpha_t \mathbf{x}_0, \sigma_t^2 \mathbf{I}) \quad (1)$$

where α_t and σ_t is the noise coefficient. We can quickly sample \mathbf{x}_t at arbitrary timestep by reparameterization trick. And for the reverse process, given two timesteps s and t , where $s > 0$ and $t < s$, \mathbf{x}_t is calculated as[36]:

$$\mathbf{x}_t = \frac{\alpha_t}{\alpha_s} \mathbf{x}_s - \alpha_t \int_{\lambda_s}^{\lambda_t} e^{-\lambda} \hat{\epsilon}_{\theta}(\mathbf{x}_{t_{\lambda}(\lambda)}, t_{\lambda}(\lambda)) d\lambda \quad (2)$$

where $\lambda_t = \log(\alpha_t/\sigma_t)$. $t_{\lambda}(\lambda)$ is the inverse function of λ_t that satisfies $t_{\lambda}(\lambda_t) = t$. $\epsilon_{\theta}(\cdot)$ often represents the learned model, which, in our case, is the diffusion transformer. Previous methods

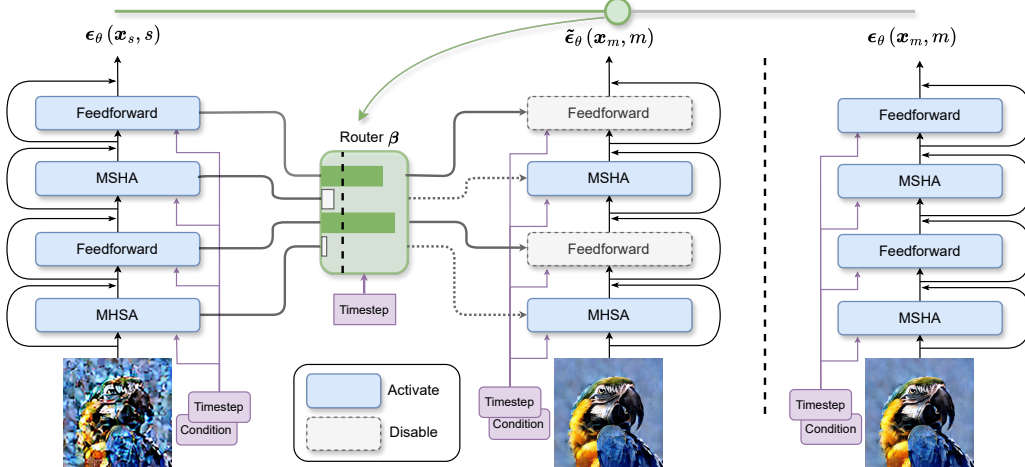


Figure 2: Illustration of Learning-to-Cache. When a layer is activated, the calculation proceeds as usual. In contrast, when a layer is disabled, the computation of the non-residual path is bypassed, and the results from the previous step are utilized instead. The router β smoothly controls the transition between two endpoints $\epsilon_\theta(\mathbf{x}_s, s)$ and $\epsilon_\theta(\mathbf{x}_m, m)$.

show that this integral term can be approximated by adopting Taylor expansion at λ_s , adopting the first-order [57] or higher-order approximation of this [36]. Take the first-order one as an example, the update of \mathbf{x}_t would be:

$$\mathbf{x}_t = \frac{\alpha_t}{\alpha_s} \mathbf{x}_s - \sigma_t (e^{\lambda_t - \lambda_s} - 1) \epsilon_\theta(\mathbf{x}_s, s) \quad (3)$$

3.2 Approximating $\epsilon_\theta(\cdot)$ with a lightweight substitute

The question falls into how to efficiently calculate the term $\int_{\lambda_s}^{\lambda_t} e^{-\lambda} \tilde{\epsilon}_\theta(\mathbf{x}_{t_\lambda(\lambda)}, t_\lambda(\lambda)) d\lambda$. Our core idea is that we want to keep more updates between s and t while the overall inference time would not increase too much. Suppose that we have three timesteps: s and t and one step m between s and t , the calculation of \mathbf{x}_t , in the case of Eq.3, would become:

$$\mathbf{x}_t = \frac{\alpha_t}{\alpha_m} \mathbf{x}_m - \sigma_t (e^{\lambda_t - \lambda_m} - 1) \epsilon_\theta(\mathbf{x}_m, m), \text{ where } \mathbf{x}_m = \frac{\alpha_m}{\alpha_s} \mathbf{x}_s - \sigma_m (e^{\lambda_m - \lambda_s} - 1) \epsilon_\theta(\mathbf{x}_s, s) \quad (4)$$

If we directly set $\epsilon_\theta(\mathbf{x}_m, m) = \epsilon_\theta(\mathbf{x}_s, s)$, it would be equivalent to the results in Equation 3 if we take a step directly from s to t (see the derivation in Appendix A.1). This approach results in faster computation, as it eliminates the need to compute $\epsilon_\theta(\mathbf{x}_m, m)$; however, it compromises the quality of the resulting image. In contrast, another time-consuming but optimal way is to calculate $\epsilon_\theta(\mathbf{x}_m, m)$ as usual, which necessitates a full model evaluation but yields superior image quality.

Recognizing that $\epsilon_\theta(\mathbf{x}_s, s)$ represents a rapid yet suboptimal solution and $\epsilon_\theta(\mathbf{x}_m, m)$ represents a slower but optimal solution when calculating \mathbf{x}_t , we want to find a model $\tilde{\epsilon}(\mathbf{x}_m, m)$, which is the interpolation of these two models. We first define the interpolation as follows:

$$\tilde{\epsilon}_\theta(\mathbf{x}_m, m; \beta) = \mathcal{I}(\epsilon_\theta(\mathbf{x}_s, s), \epsilon_\theta(\mathbf{x}_m, m), \beta) \quad (5)$$

where $\tilde{\epsilon}_\theta(\mathbf{x}_m, m)$ is controlled by a set of variables β , functioning as a slider that can smoothly transition between the two endpoints $\epsilon_\theta(\mathbf{x}_s, s)$ and $\epsilon_\theta(\mathbf{x}_m, m)$. $\tilde{\epsilon}_\theta(\mathbf{x}_m, m)$ needs to meet two criteria: it should approximate the output of $\epsilon_\theta(\mathbf{x}_m, m)$ and be faster for inference compared to $\epsilon_\theta(\mathbf{x}_m, m)$. By creating the interpolation \mathcal{I} , we generate a large collection of models, allowing us to search within this set to find if there exists an $\tilde{\epsilon}_\theta(\mathbf{x}_m, m)$ that satisfies our requirements.

3.3 Caching the Layer: A Feasible Choice for the Interpolation \mathcal{I}

In this section, we specifically define an interpolation \mathcal{I} and explore the possibility of the existence of $\tilde{\epsilon}_\theta(\mathbf{x}_m, m)$ within it. Given the transformer architecture, we propose an interpolation schema

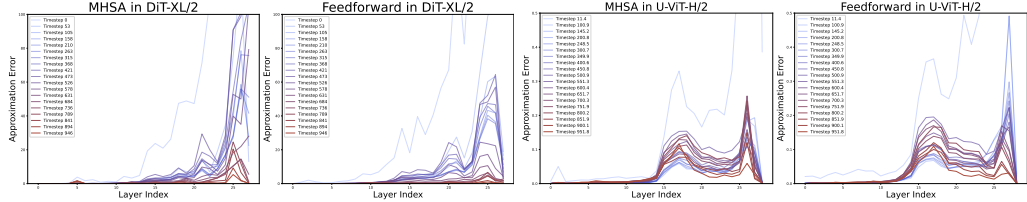


Figure 3: Approximation Error for DiT and U-ViT in different timesteps and different layers

by leveraging the layers of the transformer model. Here we take the computation of DiT[46] as an illustrative example. The transformer model can be decomposed into a sequence of basic layers $L_i(h, t)_{i=1}^D$, where $L_i(h, t) = h + g(t) * f_i(h, t)$, consisting of a residual connection. Here, h is the input feature, and D denotes the depth of the model. t is the time condition. $f_i(h, t)$ can represent either a multi-head self-attention (MHSA) block or a pointwise feedforward block, and $g(t)$ is a time-conditioned scalar. We omit the condition t in $f_i(h, t)$ for simplicity. Then we can construct a linear interpolation within the layers, and this interpolation of layer satisfies the model interpolation \mathcal{I} (See Appendix A.2):

$$\tilde{L}_i(h_i^m, m; \alpha_i, \beta_i) = h_i^m - (1 - \alpha_i) \cdot (h_i^m - h_i^s) + g(m) (\beta_i \cdot f(h_i^m) + (1 - \beta_i) \cdot f(h_i^s)) \quad (6)$$

where h_i^s and h_i^m is the input to the block L_i at timestep s and m respectively. β_i is a coefficient in layer i to control the proximity to $f(h_i^m)$ or $f(h_i^s)$ and α_i is used as a control for the input. Both of these variables are constrained within the range $[0, 1]$.

This interpolation provides a special mechanism for inference. If β_i in layer i is set to 0, the output can be directly taken from the layer in the previous timestep, allowing the computation cost in this layer to be skipped. Non-zero β_i would trigger the original computation of layer i . A discretized β_i can be seen as a router, which selects the layers to be activated or disabled. And for α_i , it can be set to any value since there is almost no computation cost for a combination of h_i^m and h_i^s and we choose $\alpha_i = 0$. By setting more β_i in different layers to 0, the acceleration ratio can be cumulative. Therefore, we can calculate the total computational cost based on the number of non-zero β_i , and our goal $\tilde{\epsilon}_\theta(\mathbf{x}_m, m)$ can be interpreted as finding as many zeros in $\{\beta_i\}_{i=1}^D$ as possible with the minimal approximation error between $\tilde{\epsilon}_\theta(\mathbf{x}_m, m)$ and $\epsilon_\theta(\mathbf{x}_m, m)$.

One key observation. One greedy way for finding the β_i in each layer is taking the approximation error of each layer into account:

$$E = \|\tilde{L}(\cdot) - L(\cdot)\|_2^2 = (1 - \beta_i) \cdot |g(m)| \cdot \|f(h_i^m) - f(h_i^s)\|_2^2 \quad (7)$$

and taking β_i in those layer with smallest $|g(m)| \cdot \|f(h_i^m) - f(h_i^s)\|_2^2$ to be 0. In Figure 3, we analyze $\|f(h_i^m) - f(h_i^s)\|_2^2$ in two types of models: DiT and U-ViT. We find that performance varies significantly across different timesteps, even at the same layer. Particularly in the DiT model, the error is markedly higher in the later steps compared to the early denoising steps. Additionally, the performance of multi-head self-attention differs substantially from that of feedforward layers. Based on this, we assign each timestep with its own $\{\beta_i\}_{i=1}^D$. Thus, β becomes time-variant, where $\beta = \{\beta_{ij} \mid i = 1, 2, \dots, T; j = 1, 2, \dots, D\}$ and T is the total denoising steps.

In addition, we directly use this metric as the criterion for β_{ij} and employ it during inference. From the experimental results in 4, we observe that it cannot effectively handle a combination of layers. This limitation arises because the approximation error for each layer is influenced by changes in the preceding layer. However, exhaustively evaluating all possible configurations is impractical, as the number of trials increases exponentially with the depth of the model.

3.4 Learning to Cache

To address this, we propose the following method: Learning to Cache. Recall that our goal is to find a $\tilde{\epsilon}_\theta(\mathbf{x}_m, m)$ that is (1) as close as $\epsilon_\theta(\mathbf{x}_m, m)$ and (2) with minimal computation cost. We can reformulate this as an optimization problem as:

$$\arg \min_{\beta} \|\tilde{\epsilon}(\mathbf{x}_m, m; \beta) - \epsilon(\mathbf{x}_m, m)\|_2^2 \quad \text{s.t. } \sum_{i=1}^D \delta_{\beta_{ij}, 1} \leq C \quad (8)$$

Algorithm 1 Training

```
1: Input: Data distribution  $p(\mathbf{x}_0)$ , diffusion model  
    $\epsilon_\theta(\cdot)$ , learning rate  $\eta$ , ODE solver  $\Psi(\cdot)$ , total steps  
    $T$  and the step schedule  $\{t_i\}_{i=1}^T$  in  $\Psi(\cdot)$   
2:  $\beta \sim \mathcal{N}(0, 1)$   
3: repeat  
4:    $\mathbf{x}_0 \sim p(\mathbf{x}_0), n \sim \mathcal{U}[1, T/2]$   
   // Step s for calculating states for caching  
5:    $s \leftarrow t_{n*2}$   
6:    $\mathbf{x}_s \sim \mathcal{N}(\mathbf{x}_s; \alpha_s \mathbf{x}_0, \sigma_s^2 \mathbf{I})$   
7:    $\epsilon_s \leftarrow \epsilon_\theta(\mathbf{x}_s, s)$  and cache  $\{f(\cdot)\}_{i=1}^D$   
   // Step m for using cached states  
8:    $m \leftarrow t_{n*2-1}$   
9:    $\mathbf{x}_m \leftarrow \Psi(\epsilon_s, s, m)$   
10:   $\beta_m \leftarrow \text{Sigmoid}(\beta_m)$   
   // Optimize  
11:  Calculate  $\tilde{\epsilon}(\mathbf{x}_m, m; \beta_m)$  by Eq.6  
12:   $\mathcal{L} \leftarrow \|\tilde{\epsilon}(\mathbf{x}_m, m) - \epsilon_\theta(\mathbf{x}_m, m)\|_2^2 + \lambda \sum \beta_m$   
13:   $\beta_m \leftarrow \beta_m - \eta \nabla_{\beta_m} \mathcal{L}$   
14: until converged
```

Algorithm 2 Sampling

```
1: Input: Diffusion model  $\epsilon_\theta(\cdot)$ , router  $\beta$ , ODE  
   solver  $\Psi(\cdot)$ , threshold  $\theta$ , total steps  $T$  and the  
   step schedule  $\{t_i\}_{i=1}^T$  in  $\Psi(\cdot)$   
2:  $\mathbf{x}_T \sim \mathcal{N}(\mathbf{0}, \mathbf{I})$   
3: for  $n = T, \dots, 1$  do  
4:    $h_1^{t_n} \leftarrow \mathbf{x}_n$   
5:   for  $i = 1, \dots, D$  do  
6:     if  $\text{Sigmoid}(\beta_{t_n i}) > \theta$  and step  $n$  is the  
       cache step then  
7:        $\beta_i \leftarrow 0$   
8:     else  
9:        $\beta_i \leftarrow 1$   
10:    end if  
11:     $h_{i+1}^{t_n} \leftarrow \tilde{\epsilon}(h_i^{t_n}, t_n; 0, \beta_i)$  by Eq.6  
12:   end for  
13:    $\tilde{\epsilon}(x_n, t_n) \leftarrow h_{D+1}^{t_n}$   
14:    $\mathbf{x}_{n-1} \leftarrow \Psi(\tilde{\epsilon}(\mathbf{x}_n, t_n), t_n, t_{n-1})$   
15: end for  
16: return  $\mathbf{x}_0$ 
```

where C is the constraint for the total cost. $\delta_{\beta_{ij}, 1}$ is the Kronecker delta function, which is 1 if $\beta_{ij} = 1$. Though β_{ij} in the final solution needs to be discrete, β_{ij} is designed to be continuous to make the computation differentiable when optimized. And when inference, a threshold θ would be set to discretize the β_{ij} to be either 0 or 1, where β_{ij} turned to become a router. The only trained variables in our algorithm are β . Thus, the parameters in the diffusion model would remain unchanged. With the help of Lagrange duality to transform the optimization problem into an unconstrained one, the loss would be:

$$\mathcal{L}(\tilde{\epsilon}, \epsilon, \mathbf{x}_m, m; \beta) = \|\tilde{\epsilon}(\mathbf{x}_m, m; \beta) - \epsilon(\mathbf{x}_m, m)\|_2^2 + \lambda \cdot \sum_{i=1}^D \beta_{ij} \quad (9)$$

where λ is the Lagrangian multiplier that governs the regularization. We show the algorithm for training and inference in Algorithm 1 and 2. To ensure β remains within the range $[0, 1]$, a sigmoid operation is performed before β is passed into the model. In these algorithms, we adopt layer caching every two steps, representing that only half of the steps would inference in a faster speed. For simplicity, the image encoder and decoder are omitted.

4 Experiments

4.1 Experimental Setup

Models and Datasets. We explore our methods on two commonly used transformer architectures in diffusion models: DiT [46] and U-ViT [3]. Specifically, we use DiT-XL/2 (256×256), DiT-XL/2 (512×512), DiT-L/2 and U-ViT-H/2. Except for DiT-L/2, we use the officially released models. We trained a DiT-L/2 for one million steps, which is used to investigate if layer redundancy exists in smaller models that may not be fully converged. Most of the results are presented under the resolution 256×256 and we also show the results on models that generate high resolution 512×512 images.

Implementations. Since the parameters of the diffusion model would not be updated, the only parameters that require optimization are β , resulting in a very limited number of variables. For example, for DiT-XL-2 with 20 denoising steps, the number of trainable variables is 560. We take the training set of ImageNet to train β for 1 epoch. The learning rate is set to 0.01 and AdamW optimizer is used to optimize β . The training is conducted upon 8 A5000 GPUs with a global batch size equal to 64. To train with classifier-free guidance, we randomly drop some labels and assign a null token to the label. The dropping rates for labels follow the original training pipeline.

Table 1: Accelerating image generation on ImageNet for the DiT model family.

Methods	NFE	MACs(T)	Latency(s)	Speedup	IS↑	FID↓	sFID↓	Precision↑	Recall↑
DiT-XL/2 (ImageNet 256×256) (cfg=1.5)									
DDPM	250	28.61	36.55	-	280.1	2.27	4.54	82.73	57.95
DDIM	250	28.61	36.45	-	243.4	2.14	4.55	80.70	60.57
DDIM	50	5.72	7.25	1.00×	238.6	2.26	4.29	80.16	59.89
DDIM	40	4.57	5.82	1.24×	239.8	2.39	4.28	80.36	59.13
Ours	50	4.36	5.57	1.30×	244.1	2.27	4.23	80.94	58.76
DDIM	20	2.29	2.87	1.00×	223.5	3.48	4.89	78.76	57.07
DDIM	16	1.83	2.30	1.25×	210.9	4.68	5.71	76.78	56.20
Ours	20	1.78	2.26	1.27×	227.0	3.46	4.64	79.15	55.62
DDIM	10	1.14	1.43	1.00×	158.3	12.38	11.22	66.78	52.82
DDIM	9	1.03	1.29	1.11×	140.9	16.57	14.21	62.28	49.98
Ours	10	1.04	1.30	1.10×	156.3	12.79	10.42	66.21	52.15
DiT-XL/2 (ImageNet 512×512) (cfg=1.5)									
DDIM	50	22.85	37.73	1.00×	204.1	3.28	4.50	83.33	54.80
DDIM	30	13.71	22.51	1.68×	198.3	3.85	4.92	83.01	56.00
Ours	50	14.19	22.57	1.67×	202.1	3.69	5.03	82.90	54.60
DiT-L/2 (ImageNet 256×256) (cfg=1.5)									
DDIM	50	3.88	5.06	1.00×	167.6	4.82	4.40	78.72	54.66
DDIM	40	3.10	4.06	1.25×	168.2	4.99	4.43	79.01	54.71
Ours	50	2.95	4.01	1.26×	168.3	4.82	4.41	78.97	54.73
DDIM	20	1.55	2.01	1.00×	160.16	6.45	5.26	77.13	53.65
DDIM	16	1.24	1.63	1.23×	151.70	7.91	6.24	75.93	51.71
Ours	20	1.20	1.60	1.26×	160.53	6.55	5.08	77.47	52.22

Table 2: Results with U-ViT-H/2 on ImageNet dataset. The resolution here is 256×256. We adopt the DPM-Solver-2, which has 2 function evaluations per step. The total NFE (instead of steps) is reported below. Guidance strength is set to 0.4.

Methods		NFE	MACs	Latency	Speedup		NFE	MACs	Latency	Speedup		FID↓
DPM-Solver		50	6.44	19.37	1.00×		20	2.58	7.69	1.00×		2.5739
DPM-Solver		30	3.86	11.55	1.68×		16	2.06	6.08	1.26×		2.7005
Ours		50	3.79	11.16	1.74×		20	1.92	5.64	1.35×		2.5809

Evaluation. We tested our method upon two samplers, DDIM[57] and DPM-Solver[36], with sampling steps from 10 to 50. For the DiT model, we use the DDIM sampler. And for U-ViT, we use the DPM-Solver-2. All the experiments here use classifier-free guidance. To evaluate the image quality, 50k images are generated per trial. We measure the image quality with Frechet Inception Distance(FID)[43], sFID[43], Inception Score[51], Precision and Recall[26]. Besides, we reported the total MACs and the latency to make a comparison of the acceleration ratio. The MACs is evaluated using pytorch-OpCounter², and the latency is tested when generating a batch of images(8 images) with classifier-free guidance on a single A5000, which we conducted five tests and took the average.

4.2 Main Results

We present the results of DiT in Tables 1 and 2, comparing our algorithms with samplers of comparable inference speed. Our method requires more denoising steps, but each step takes less average time. In contrast, samplers require fewer steps, but each step takes more time. Our experiments demonstrate that our methods significantly outperform DDIM and DPM-Solver. For instance, with the 20-step DDIM on DiT-XL/2, our method achieves an FID of 3.46, nearly identical to the unaccelerated one. In comparison, the DDIM achieves an FID of 4.68. When generating high-resolution images, sampling with fewer steps, or using a relatively smaller model, our method still outperforms baselines.

²<https://github.com/Lyken17/pytorch-OpCounter>

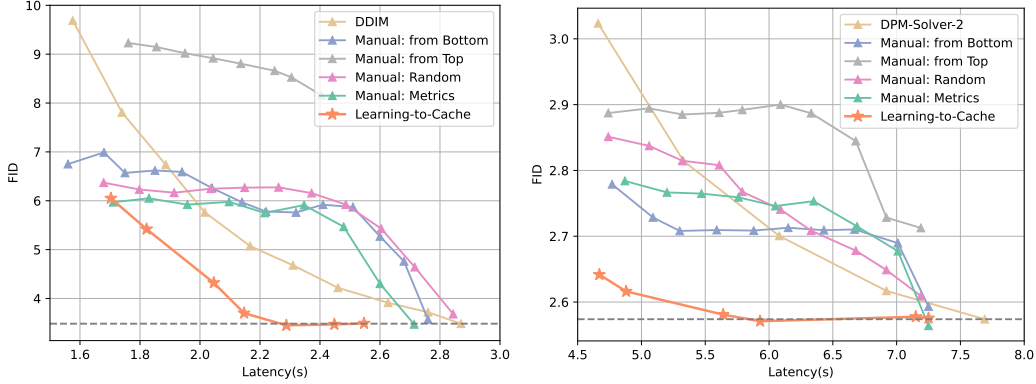


Figure 4: Speed-Quality Tradeoff for DiT-XL/2 and U-ViT-H/2 with 20 denoising steps as the basis. The dashed line indicates the performance without applying inference acceleration.

Table 3: Comparison with other cache-based method on U-ViT

Methods	NFE	Latency	Speedup	FID \downarrow
DPM-Solver	20	7.69	1.00 \times	2.57
DeepCache[40]	20	4.68	1.64 \times	2.70
Ours	20	4.62	1.67 \times	2.64
Faster Diffusion[28]	20	5.95	1.29 \times	2.82
Ours	20	5.93	1.30 \times	2.57

Table 4: Maximum cacheable layers for DiT and U-ViT with different steps.

Model	DiT-XL/2		U-ViT-H/2		
	NFE	50	20	50	20
Remove Ratio		47.43%	44.29%	93.68%	63.79%
FFN Remove Ratio		47.85%	44.64%	94.11%	60.54%
MHSA Remove Ratio		47.00%	43.93%	93.25%	67.05%

However, we observe that achieving nearly lossless compression under these conditions is challenging. We argue that this difficulty arises because layer redundancy is less apparent in these scenarios.

Quality-Latency Tradeoff. We show the trade-off curve between FID and Latency in Figure 4. These figures offer a more comprehensive comparison with two types of baselines: (1) **Heuristic Methods for Selecting Layers.** We designed several methods for selecting layers to cache, including rule-based approaches such as caching from top to bottom or from bottom to top, randomly selecting layers, and metric-based selection as described in Eq.7. We found that when the dependency between layers must be considered, they fail to select the optimal layers, leading to a degradation in image quality. In contrast, our method consistently achieves improved quality across various acceleration ratios. (2) **Sampler with fewer steps.** Our method significantly outperforms DDIM and DPM-Solver, as evidenced by the detailed comparison provided.

Maximum Cacheable Layers for diffusion transformer. From the trade-off curve, we found that there exists an upper limit for the number of cacheable layers. Below this limit, image quality remains almost unaffected, as indicated by a FID degradation of less than 0.01. This limit is detailed in Table 4. Notably, caching does not occur at every step: step s involves full model inference, while only step m caches layers. With a significant proportion of layers can be cached and the computation of these layers to be saved, notable differences emerge between the U-ViT and DiT models. For instance, in U-ViT, up to 94% of layers can be discarded for the cache step during the denoising process, whereas this proportion is considerably lower for DiT. Furthermore, we observed that the cacheable ratios for FFN and MHSA vary.

Comparison with other cache-based methods We also compared our method with other cache-based methods. Notably, previous cache-based methods are strongly coupled to the U-Net structure and cannot be applied to models without the U-structure, such as DiT. To ensure a fair comparison, we selected U-ViT, which incorporates both the U-structure and transformers, to implement these methods as baselines alongside our method. Table 3 presents the comparison results. The findings demonstrate that our method achieves better quality than the baselines.

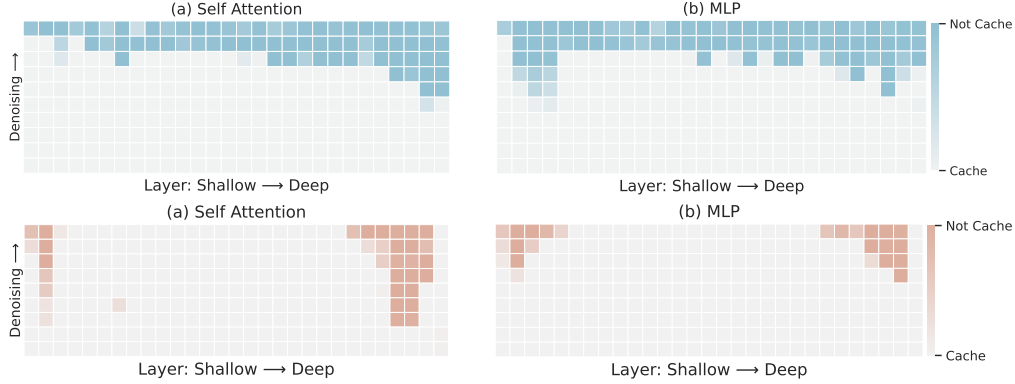


Figure 5: Learned Router β for DiT-XL/2 (Top) and U-ViT-H/2 (Bottom). Different caching patterns are observed in different types of diffusion transformers.

Table 5: Comparison with layer dropout. The removal ratio corresponds to the percentage of sub-layers being removed, including both MHSA and MLP blocks, for a total of 28 layers and 10 steps.

Methods	Remove Ratio	Latency(s)	Speedup	IS↑	FID↓	sFID↓	Precision↑	Recall↑
Random Drop	170/560	2.439	1.18×	3.36	277.42	171.83	1.23	0.24
Learning-to-Drop	179/560	2.421	1.19×	113.93	17.35	28.46	60.25	52.68
Learning-to-Cache	176/560	2.438	1.18×	226.13	3.47	4.58	79.19	56.47

4.3 Analysis

The Learned Pattern of β We present the learned pattern in Figure 5. The two different architectures produce distinct patterns. For U-ViT, the entire middle section is almost entirely cacheable, allowing it to be replaced with the results from the previous step’s calculations. However, the computations at both ends of the model are crucial and cannot be discarded. This observation explains why DeepCache outperforms faster-diffusion on U-ViT, as the learned patterns resemble the manually designed approach of DeepCache. However, this phenomenon is not clearly observed in DiT-XL. Additionally, we found a consistent tendency across models to retain more computation in the later stages while discarding calculations in the earlier stages. This observation aligns with our findings in Figure 3. When comparing the impact of different steps within the same layer, removing parts with smaller timestep has a greater effect on the changes in the output.

Comparison between Layer Cache and Layer Dropout Layer dropout involves directly removing $f_i(\cdot)$, retaining only the computation in the skip path. We compare our method with layer dropout, where the layers are either randomly dropped or optimized using our algorithm (named Learning-to-Drop). The results, presented in Table 5, indicate that layer caching significantly outperforms layer dropout. Interestingly, when we learn the layers to be dropped, the models still produce acceptable images, although the quality is not as high. Illustrative examples are provided in Appendix B.2.

Choice of threshold We investigated the effect of different thresholds on the image quality. Results are shown in Figure 6, where the model here is trained with six different λ (corresponding to 6 points on one curve). We show the effect of different λ in Appendix B.3. Our results reveal that for higher acceleration ratios, a larger threshold improves image quality. Conversely, for lower acceleration ratios, a smaller threshold is more effective. These findings suggest that ranking layers by importance is not a reliable approach, since the selection of layers does not follow a strict sequential order. Otherwise, one threshold would win all.

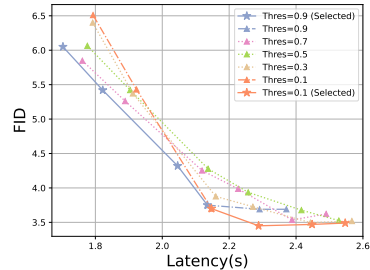


Figure 6: Effect of threshold θ .

5 Limitation

The primary limitation of this work arises from its dependence on the trained diffusion models. For instance, when applied to DiT-XL/2 at a resolution of 512, our method encounters a slight drop in FID. Although it still surpasses the baseline, this indicates that the lossless caching of the layers does not uniformly exist across all models. It highlights significant variations between different models, and thus our method is strongly dependent on the structure design of the trained diffusion models. Another limitation of our method is that the acceleration is capped at $2\times$ because every two steps consist of one full model inference step and one cheaper step. This inherently restricts the maximum achievable acceleration ratio. However, we believe that this approach can be expanded to more than two steps, potentially improving the overall efficiency.

6 Conclusion

In this paper, we propose a novel acceleration method for diffusion transformers. By interpolating between the computationally inexpensive solution but suboptimal model, and the optimal solution but expensive model, we find there exist some models which would infer much faster and also produce high-fidelity images. To find this we train the router which is continuous when training and would be discretized when inference. Experiments show that our method largely outperforms baselines such as DDIM, DPM-Solver and other cache-based methods.

Acknowledgement

This project is supported by the National Research Foundation, Singapore, under its Medium Sized Center for Advanced Robotics Technology Innovation.

References

- [1] Shubham Agarwal, Subrata Mitra, Sarthak Chakraborty, Srikrishna Karanam, Koyel Mukherjee, and Shiv Kumar Saini. Approximate caching for efficiently serving {Text-to-Image} diffusion models. In *21st USENIX Symposium on Networked Systems Design and Implementation (NSDI 24)*, pages 1173–1189, 2024.
- [2] Fan Bao, Chongxuan Li, Jun Zhu, and Bo Zhang. Analytic-dpm: an analytic estimate of the optimal reverse variance in diffusion probabilistic models. *arXiv preprint arXiv:2201.06503*, 2022.
- [3] Fan Bao, Shen Nie, Kaiwen Xue, Yue Cao, Chongxuan Li, Hang Su, and Jun Zhu. All are worth words: A vit backbone for diffusion models. In *Proceedings of the IEEE/CVF Conference on Computer Vision and Pattern Recognition*, pages 22669–22679, 2023.
- [4] Tim Brooks, Bill Peebles, Connor Holmes, Will DePue, Yufei Guo, Li Jing, David Schnurr, Joe Taylor, Troy Luhman, Eric Luhman, Clarence Ng, Ricky Wang, and Aditya Ramesh. Video generation models as world simulators. 2024.
- [5] Ziang Cao, Fangzhou Hong, Tong Wu, Liang Pan, and Ziwei Liu. Large-vocabulary 3d diffusion model with transformer. *arXiv preprint arXiv:2309.07920*, 2023.
- [6] Thibault Castells, Hyoung-Kyu Song, Bo-Kyeong Kim, and Shinkook Choi. Ld-pruner: Efficient pruning of latent diffusion models using task-agnostic insights. *arXiv preprint arXiv:2404.11936*, 2024.
- [7] Shoufa Chen, Mengmeng Xu, Jiawei Ren, Yuren Cong, Sen He, Yanping Xie, Animesh Sinha, Ping Luo, Tao Xiang, and Juan-Manuel Perez-Rua. Gentron: Delving deep into diffusion transformers for image and video generation. *arXiv preprint arXiv:2312.04557*, 2023.
- [8] Zigeng Chen, Gongfan Fang, Xinyin Ma, and Xinchao Wang. 0.1% data makes segment anything slim. *arXiv preprint arXiv:2312.05284*, 2023.
- [9] Zigeng Chen, Xinyin Ma, Gongfan Fang, Zhenxiong Tan, and Xinchao Wang. Asyncdiff: Parallelizing diffusion models by asynchronous denoising. *arXiv preprint arXiv:2406.06911*, 2024.
- [10] Prafulla Dhariwal and Alexander Nichol. Diffusion models beat gans on image synthesis. *Advances in neural information processing systems*, 34:8780–8794, 2021.
- [11] Tim Dockhorn, Arash Vahdat, and Karsten Kreis. Score-based generative modeling with critically-damped langevin diffusion. *arXiv preprint arXiv:2112.07068*, 2021.
- [12] Alexey Dosovitskiy, Lucas Beyer, Alexander Kolesnikov, Dirk Weissenborn, Xiaohua Zhai, Thomas Unterthiner, Mostafa Dehghani, Matthias Minderer, Georg Heigold, Sylvain Gelly, et al. An image is worth 16x16 words: Transformers for image recognition at scale. *arXiv preprint arXiv:2010.11929*, 2020.
- [13] Patrick Esser, Sumith Kulal, Andreas Blattmann, Rahim Entezari, Jonas Müller, Harry Saini, Yam Levi, Dominik Lorenz, Axel Sauer, Frederic Boesel, et al. Scaling rectified flow transformers for high-resolution image synthesis. In *Forty-first International Conference on Machine Learning*, 2024.
- [14] Angela Fan, Edouard Grave, and Armand Joulin. Reducing transformer depth on demand with structured dropout. In *International Conference on Learning Representations*, 2020.
- [15] Gongfan Fang, Xinyin Ma, Michael Bi Mi, and Xinchao Wang. Isomorphic pruning for vision models. *arXiv preprint arXiv:2407.04616*, 2024.
- [16] Gongfan Fang, Xinyin Ma, and Xinchao Wang. Structural pruning for diffusion models. *Advances in neural information processing systems*, 36, 2024.
- [17] Shanghua Gao, Pan Zhou, Ming-Ming Cheng, and Shuicheng Yan. Masked diffusion transformer is a strong image synthesizer. In *Proceedings of the IEEE/CVF International Conference on Computer Vision*, pages 23164–23173, 2023.
- [18] Yefei He, Luping Liu, Jing Liu, Weijia Wu, Hong Zhou, and Bohan Zhuang. Ptqd: Accurate post-training quantization for diffusion models. In A. Oh, T. Naumann, A. Globerson, K. Saenko, M. Hardt, and S. Levine, editors, *Advances in Neural Information Processing Systems*, volume 36, pages 13237–13249. Curran Associates, Inc., 2023.
- [19] Jonathan Ho, Ajay Jain, and Pieter Abbeel. Denoising diffusion probabilistic models. *Advances in neural information processing systems*, 33:6840–6851, 2020.

- [20] Rosco Hunter, Łukasz Dudziak, Mohamed S Abdelfattah, Abhinav Mehrotra, Sourav Bhattacharya, and Hongkai Wen. Fast inference through the reuse of attention maps in diffusion models. *arXiv preprint arXiv:2401.01008*, 2023.
- [21] Xin Jing, Yi Chang, Zijiang Yang, Jiangjian Xie, Andreas Triantafyllopoulos, and Bjoern W Schuller. U-dit tts: U-diffusion vision transformer for text-to-speech. In *Speech Communication; 15th ITG Conference*, pages 56–60. VDE, 2023.
- [22] Alexia Jolicoeur-Martineau, Ke Li, Rémi Piché-Taillefer, Tal Kachman, and Ioannis Mitliagkas. Gotta go fast when generating data with score-based models. *arXiv preprint arXiv:2105.14080*, 2021.
- [23] Tero Karras, Miika Aittala, Timo Aila, and Samuli Laine. Elucidating the design space of diffusion-based generative models. *Advances in Neural Information Processing Systems*, 35:26565–26577, 2022.
- [24] Bo-Kyeong Kim, Geonmin Kim, Tae-Ho Kim, Thibault Castells, Shinkook Choi, Junho Shin, and Hyoung-Kyu Song. Shortened llama: A simple depth pruning for large language models. *arXiv preprint arXiv:2402.02834*, 2024.
- [25] Bo-Kyeong Kim, Hyoung-Kyu Song, Thibault Castells, and Shinkook Choi. Bk-sdm: Architecturally compressed stable diffusion for efficient text-to-image generation. In *Workshop on Efficient Systems for Foundation Models@ ICML2023*, 2023.
- [26] Tuomas Kynkänniemi, Tero Karras, Samuli Laine, Jaakko Lehtinen, and Timo Aila. Improved precision and recall metric for assessing generative models. *Advances in neural information processing systems*, 32, 2019.
- [27] Muyang Li, Tianle Cai, Jiaxin Cao, Qinsheng Zhang, Han Cai, Junjie Bai, Yangqing Jia, Ming-Yu Liu, Kai Li, and Song Han. Distrifusion: Distributed parallel inference for high-resolution diffusion models. *arXiv preprint arXiv:2402.19481*, 2024.
- [28] Senmao Li, Taihang Hu, Fahad Shahbaz Khan, Linxuan Li, Shiqi Yang, Yaxing Wang, Ming-Ming Cheng, and Jian Yang. Faster diffusion: Rethinking the role of unet encoder in diffusion models. *arXiv preprint arXiv:2312.09608*, 2023.
- [29] Xiuyu Li, Yijiang Liu, Long Lian, Huanrui Yang, Zhen Dong, Daniel Kang, Shanghang Zhang, and Kurt Keutzer. Q-diffusion: Quantizing diffusion models. In *Proceedings of the IEEE/CVF International Conference on Computer Vision (ICCV)*, pages 17535–17545, October 2023.
- [30] Yanyu Li, Huan Wang, Qing Jin, Ju Hu, Pavlo Chemerys, Yun Fu, Yanzhi Wang, Sergey Tulyakov, and Jian Ren. Snapfusion: Text-to-image diffusion model on mobile devices within two seconds. *Advances in Neural Information Processing Systems*, 36, 2024.
- [31] Shanchuan Lin, Anran Wang, and Xiao Yang. Sdxl-lightning: Progressive adversarial diffusion distillation. *arXiv preprint arXiv:2402.13929*, 2024.
- [32] Enshu Liu, Xuefei Ning, Zinan Lin, Huazhong Yang, and Yu Wang. Oms-dpm: Optimizing the model schedule for diffusion probabilistic models. *arXiv preprint arXiv:2306.08860*, 2023.
- [33] Huadai Liu, Rongjie Huang, Xuan Lin, Wenqiang Xu, Maozong Zheng, Hong Chen, Jinzheng He, and Zhou Zhao. Vit-tts: visual text-to-speech with scalable diffusion transformer. *arXiv preprint arXiv:2305.12708*, 2023.
- [34] Luping Liu, Yi Ren, Zhijie Lin, and Zhou Zhao. Pseudo numerical methods for diffusion models on manifolds. *arXiv preprint arXiv:2202.09778*, 2022.
- [35] Songhua Liu, Weihao Yu, Zhenxiong Tan, and Xinchao Wang. Linfusion: 1 gpu, 1 minute, 16k image. *arXiv preprint arXiv:2409.02097*, 2024.
- [36] Cheng Lu, Yuhao Zhou, Fan Bao, Jianfei Chen, Chongxuan Li, and Jun Zhu. Dpm-solver: A fast ode solver for diffusion probabilistic model sampling in around 10 steps. *Advances in Neural Information Processing Systems*, 35:5775–5787, 2022.
- [37] Cheng Lu, Yuhao Zhou, Fan Bao, Jianfei Chen, Chongxuan Li, and Jun Zhu. Dpm-solver++: Fast solver for guided sampling of diffusion probabilistic models. *arXiv preprint arXiv:2211.01095*, 2022.
- [38] Haoyu Lu, Guoxing Yang, Nanyi Fei, Yuqi Huo, Zhiwu Lu, Ping Luo, and Mingyu Ding. Vdt: General-purpose video diffusion transformers via mask modeling. In *The Twelfth International Conference on Learning Representations*, 2023.

- [39] Simian Luo, Yiqin Tan, Longbo Huang, Jian Li, and Hang Zhao. Latent consistency models: Synthesizing high-resolution images with few-step inference. *arXiv preprint arXiv:2310.04378*, 2023.
- [40] Xinyin Ma, Gongfan Fang, and Xinchao Wang. Deepcache: Accelerating diffusion models for free. *arXiv preprint arXiv:2312.00858*, 2023.
- [41] Shentong Mo, Enze Xie, Ruihang Chu, Lanqing Hong, Matthias Niessner, and Zhenguo Li. Dit-3d: Exploring plain diffusion transformers for 3d shape generation. *Advances in Neural Information Processing Systems*, 36, 2024.
- [42] Taehong Moon, Moonseok Choi, EungGu Yun, Jongmin Yoon, Gayoung Lee, and Juho Lee. Early exiting for accelerated inference in diffusion models. In *ICML 2023 Workshop on Structured Probabilistic Inference \& Generative Modeling*, 2023.
- [43] Charlie Nash, Jacob Menick, Sander Dieleman, and Peter W Battaglia. Generating images with sparse representations. *arXiv preprint arXiv:2103.03841*, 2021.
- [44] Zizheng Pan, Bohan Zhuang, De-An Huang, Weili Nie, Zhiding Yu, Chaowei Xiao, Jianfei Cai, and Anima Anandkumar. T-stitch: Accelerating sampling in pre-trained diffusion models with trajectory stitching. *arXiv preprint arXiv:2402.14167*, 2024.
- [45] Zizheng Pan, Bohan Zhuang, De-An Huang, Weili Nie, Zhiding Yu, Chaowei Xiao, Jianfei Cai, and Anima Anandkumar. T-stitch: Accelerating sampling in pre-trained diffusion models with trajectory stitching, 2024.
- [46] William Peebles and Saining Xie. Scalable diffusion models with transformers. In *Proceedings of the IEEE/CVF International Conference on Computer Vision*, pages 4195–4205, 2023.
- [47] Ziheng Qin, Kai Wang, Zangwei Zheng, Jianyang Gu, Xiangyu Peng, Zhaopan Xu, Daquan Zhou, Lei Shang, Baigui Sun, Xiansong Xie, et al. Infobatch: Lossless training speed up by unbiased dynamic data pruning. *arXiv preprint arXiv:2303.04947*, 2023.
- [48] David Raposo, Sam Ritter, Blake Richards, Timothy Lillicrap, Peter Conway Humphreys, and Adam Santoro. Mixture-of-depths: Dynamically allocating compute in transformer-based language models. *arXiv preprint arXiv:2404.02258*, 2024.
- [49] Robin Rombach, Andreas Blattmann, Dominik Lorenz, Patrick Esser, and Björn Ommer. High-resolution image synthesis with latent diffusion models. In *Proceedings of the IEEE/CVF conference on computer vision and pattern recognition*, pages 10684–10695, 2022.
- [50] Olaf Ronneberger, Philipp Fischer, and Thomas Brox. U-net: Convolutional networks for biomedical image segmentation. In *Medical Image Computing and Computer-Assisted Intervention–MICCAI 2015: 18th International Conference, Munich, Germany, October 5–9, 2015, Proceedings, Part III 18*, pages 234–241. Springer, 2015.
- [51] Tim Salimans, Ian Goodfellow, Wojciech Zaremba, Vicki Cheung, Alec Radford, and Xi Chen. Improved techniques for training gans. *Advances in neural information processing systems*, 29, 2016.
- [52] Tim Salimans and Jonathan Ho. Progressive distillation for fast sampling of diffusion models. *arXiv preprint arXiv:2202.00512*, 2022.
- [53] Yuzhang Shang, Zhihang Yuan, Bin Xie, Bingzhe Wu, and Yan Yan. Post-training quantization on diffusion models. In *Proceedings of the IEEE/CVF Conference on Computer Vision and Pattern Recognition*, pages 1972–1981, 2023.
- [54] Andy Shih, Suneel Belkhale, Stefano Ermon, Dorsa Sadigh, and Nima Anari. Parallel sampling of diffusion models. *arXiv preprint arXiv:2305.16317*, 2023.
- [55] Alan Jay Smith. Cache memories. *ACM Computing Surveys (CSUR)*, 14(3):473–530, 1982.
- [56] Junhyuk So, Jungwon Lee, and Eunhyeok Park. Frdiff: Feature reuse for exquisite zero-shot acceleration of diffusion models. *arXiv preprint arXiv:2312.03517*, 2023.
- [57] Jiaming Song, Chenlin Meng, and Stefano Ermon. Denoising diffusion implicit models. *arXiv preprint arXiv:2010.02502*, 2020.
- [58] Yang Song, Prafulla Dhariwal, Mark Chen, and Ilya Sutskever. Consistency models. *arXiv preprint arXiv:2303.01469*, 2023.

- [59] Yang Song and Stefano Ermon. Generative modeling by estimating gradients of the data distribution. *Advances in neural information processing systems*, 32, 2019.
- [60] Yang Song, Jascha Sohl-Dickstein, Diederik P Kingma, Abhishek Kumar, Stefano Ermon, and Ben Poole. Score-based generative modeling through stochastic differential equations. *arXiv preprint arXiv:2011.13456*, 2020.
- [61] Zhenxiong Tan, Xinyin Ma, Gongfan Fang, and Xinchao Wang. Litefocus: Accelerated diffusion inference for long audio synthesis. *arXiv preprint arXiv:2407.10468*, 2024.
- [62] Ashish Vaswani, Noam Shazeer, Niki Parmar, Jakob Uszkoreit, Llion Jones, Aidan N Gomez, Łukasz Kaiser, and Illia Polosukhin. Attention is all you need. *Advances in neural information processing systems*, 30, 2017.
- [63] Kafeng Wang, Jianfei Chen, He Li, Zhenpeng Mi, and Jun Zhu. Sparsedm: Toward sparse efficient diffusion models, 2024.
- [64] Felix Wimbauer, Bichen Wu, Edgar Schoenfeld, Xiaoliang Dai, Ji Hou, Zijian He, Artsiom Sanakoyeu, Peizhao Zhang, Sam Tsai, Jonas Kohler, et al. Cache me if you can: Accelerating diffusion models through block caching. *arXiv preprint arXiv:2312.03209*, 2023.
- [65] Shuai Yang, Yukang Chen, Luozhou Wang, Shu Liu, and Yingcong Chen. Denoising diffusion step-aware models. *arXiv preprint arXiv:2310.03337*, 2023.
- [66] Xingyi Yang and Xinchao Wang. Hash3d: Training-free acceleration for 3d generation. *arXiv preprint arXiv:2404.06091*, 2024.
- [67] Xingyi Yang, Daquan Zhou, Jia Shi Feng, and Xinchao Wang. Diffusion probabilistic model made slim. In *Proceedings of the IEEE/CVF Conference on Computer Vision and Pattern Recognition*, pages 22552–22562, 2023.
- [68] Xiulong Yang, Sheng-Min Shih, Yinlin Fu, Xiaoting Zhao, and Shihao Ji. Your vit is secretly a hybrid discriminative-generative diffusion model. *arXiv preprint arXiv:2208.07791*, 2022.
- [69] Runpeng Yu, Songhua Liu, Xingyi Yang, and Xinchao Wang. Distribution shift inversion for out-of-distribution prediction. In *Proceedings of the IEEE/CVF Conference on Computer Vision and Pattern Recognition*, pages 3592–3602, 2023.
- [70] Runpeng Yu and Xinchao Wang. Neural lineage. In *Proceedings of the IEEE/CVF Conference on Computer Vision and Pattern Recognition*, pages 4797–4807, 2024.
- [71] Dingkun Zhang, Sijia Li, Chen Chen, Qingsong Xie, and Haonan Lu. Laptop-diff: Layer pruning and normalized distillation for compressing diffusion models. *arXiv preprint arXiv:2404.11098*, 2024.
- [72] Qinsheng Zhang and Yongxin Chen. Fast sampling of diffusion models with exponential integrator. *arXiv preprint arXiv:2204.13902*, 2022.
- [73] Qinsheng Zhang, Molei Tao, and Yongxin Chen. gddim: Generalized denoising diffusion implicit models. *arXiv preprint arXiv:2206.05564*, 2022.
- [74] Wentian Zhang, Haozhe Liu, Jinheng Xie, Francesco Faccio, Mike Zheng Shou, and Jürgen Schmidhuber. Cross-attention makes inference cumbersome in text-to-image diffusion models, 2024.
- [75] Yang Zhao, Yanwu Xu, Zhisheng Xiao, and Tingbo Hou. Mobilediffusion: Subsecond text-to-image generation on mobile devices. *arXiv preprint arXiv:2311.16567*, 2023.
- [76] Hongkai Zheng, Weili Nie, Arash Vahdat, and Anima Anandkumar. Fast training of diffusion models with masked transformers. *arXiv preprint arXiv:2306.09305*, 2023.

A Proof

A.1 Two equivalent solutions to obtain \mathbf{x}_t

To get the solution of \mathbf{x}_t , the following two approaches yield equivalent results:

1. Directly update \mathbf{x}_t from \mathbf{x}_s . By the definition, the solution at time t would be:

$$\mathbf{x}_t = \frac{\alpha_t}{\alpha_s} \mathbf{x}_s - \sigma_t (e^{\lambda_t - \lambda_s} - 1) \epsilon_\theta (\mathbf{x}_s, s) \quad (10)$$

2. First compute \mathbf{x}_m from \mathbf{x}_s , and then compute \mathbf{x}_t from \mathbf{x}_m with $\epsilon_\theta (\mathbf{x}_m, m) = \epsilon_\theta (\mathbf{x}_s, s)$

Proof. First, we consider the solution of \mathbf{x}_m from \mathbf{x}_s :

$$\mathbf{x}_m = \frac{\alpha_m}{\alpha_s} \mathbf{x}_s - \sigma_m (e^{\lambda_m - \lambda_s} - 1) \epsilon_\theta (\mathbf{x}_s, s) \quad (11)$$

And for the calculation of \mathbf{x}_t with $\epsilon_\theta (\mathbf{x}_m, m) = \epsilon_\theta (\mathbf{x}_s, s)$, we have

$$\begin{aligned} \mathbf{x}_t &= \frac{\alpha_t}{\alpha_m} \mathbf{x}_m - \sigma_t (e^{\lambda_t - \lambda_m} - 1) \epsilon_\theta (\mathbf{x}_m, m) \\ &= \frac{\alpha_t}{\alpha_m} \left(\frac{\alpha_m}{\alpha_s} \mathbf{x}_s - \sigma_m (e^{\lambda_m - \lambda_s} - 1) \epsilon_\theta (\mathbf{x}_s, s) \right) - \sigma_t (e^{\lambda_t - \lambda_m} - 1) \epsilon_\theta (\mathbf{x}_s, s) \\ &= \frac{\alpha_t}{\alpha_s} \mathbf{x}_s - \left(\frac{\alpha_t}{\alpha_m} \sigma_m (e^{\lambda_m - \lambda_s} - 1) + \sigma_t (e^{\lambda_t - \lambda_m} - 1) \right) \epsilon_\theta (\mathbf{x}_s, s) \end{aligned} \quad (12)$$

Note that $\lambda_t = \log(\alpha_t/\sigma_t)$. We obtain:

$$\begin{aligned} \mathbf{x}_t &= \frac{\alpha_t}{\alpha_s} \mathbf{x}_s - \left(\frac{\alpha_t}{\alpha_m} \sigma_m \left(\frac{\alpha_m}{\sigma_m} \frac{\sigma_s}{\alpha_s} - 1 \right) + \sigma_t \left(\frac{\alpha_t}{\sigma_t} \frac{\sigma_m}{\alpha_m} - 1 \right) \right) \epsilon_\theta (\mathbf{x}_s, s) \\ &= \frac{\alpha_t}{\alpha_s} \mathbf{x}_s - \left(\alpha_t \frac{\sigma_s}{\alpha_s} - \sigma_t \right) \epsilon_\theta (\mathbf{x}_s, s) = \frac{\alpha_t}{\alpha_s} \mathbf{x}_s - \sigma_t (e^{\lambda_t - \lambda_s} - 1) \epsilon_\theta (\mathbf{x}_s, s) \end{aligned} \quad (13)$$

A.2 Layer interpolation and Interpolation \mathcal{I}

We next show that the following interpolation of the layer would satisfy the interpolation \mathcal{I} between $\epsilon_\theta (\mathbf{x}_s, s)$ and $\epsilon_\theta (\mathbf{x}_m, m)$ as we define:

$$\tilde{L}_i(h_i^m, m) = h_i^m - (1 - \alpha_i) \cdot (h_i^m - h_i^s) + g(m) (\beta_i \cdot f(h_i^m) + (1 - \beta_i) \cdot f(h_i^s)) \quad (14)$$

To prove this, we need to show these three things: (1) Interpolation condition, where the function passes through the given two models $\epsilon_\theta (\mathbf{x}_s, s)$ and $\epsilon_\theta (\mathbf{x}_m, m)$; (2) Continuity, where the interpolation function is continuous and (3) Differentiability, where the function is differentiable. Since β_i and α_i are continuous and the model also satisfies these conditions, the only thing that needs to be proved is the first property.

Proof. We show Eq.14 satisfies the interpolation condition of \mathcal{I}

- With $\{\alpha_i\}_{i=1}^D$ and $\{\beta_i\}_{i=1}^D$ set to 0, the output of the transformer would be $\epsilon_\theta (\mathbf{x}_s, s)$
If for $i \in (1, D)$, $\alpha_i = 0$ and $\beta_i = 0$ then

$$\tilde{L}_i(h_i^m, m) = h_i^s + g(m) \cdot f(h_i^s) \quad (15)$$

The output of the transformer after D layer is given by:

$$\tilde{L}_D \left(\tilde{L}_{D-1} \left(\dots \tilde{L}_1 (\mathbf{x}_s, s) \dots \right) \right) = \epsilon_\theta (\mathbf{x}_s, s) \quad (16)$$

Therefor, we get $\epsilon_\theta (\mathbf{x}_s, s)$, one of the endpoint in the interpolation \mathcal{I} .

- With $\{\alpha_i\}_{i=1}^D$ and $\{\beta_i\}_{i=1}^D$ set to 1, the output would be $\epsilon_\theta (\mathbf{x}_m, m)$. If for $i \in (1, D)$, $\alpha_i = 1$ and $\beta_i = 1$ then

$$\tilde{L}_i(h_i^m, m) = h_i^m + g(m) \cdot f(h_i^m) \quad (17)$$

The same as above, we would get $\epsilon_\theta (\mathbf{x}_m, m)$, the other endpoint in the interpolation \mathcal{I} .

B Additional Experiments

B.1 Shifted cache step for DPM-Solver

Table 6: DPM-Solver with and without Shifted Cache Steps. Here we cache all the layers.

Method	NFE	Latency	Speedup	IS	FID	sFID	Precision	Recall
DPM-Solver-2	20	7.69	1.00×	263.76	2.57	5.01	82.77	55.71
Cache	20	4.25	1.81×	222.64	5.30	7.87	76.17	54.59
Cache - shifted	20	4.54	1.70×	254.48	2.80	4.70	81.14	55.48

One important trick used in our experiment with DPM-Solver involves shifting the cache step. Specifically, when employing DPM-Solver-2, the cache steps (step here is the model evaluation) are shifted from $[2,4,6,8,10,\dots]$ to $[3,5,7,9,11,\dots]$. This adjustment is necessary because the DPM-Solver-2 requires the first-order derivative of the model $\epsilon_\theta(\cdot)$ at the current timestep, which is computed by subtracting the output at timestep i from the output at timestep $i + 1$. If the cache steps were taken at timestep $i + 1$, it would result in an incorrect estimation of the derivative. By shifting the cache step, we ensure the accurate calculation of the derivative of $\epsilon_\theta(\cdot)$. This adjustment significantly impacts the results, as demonstrated in Table 6.

B.2 Layer Dropout v.s. Layer Cache

Here we present further comparisons between layer dropout and layer caching. As illustrated in Figure 7, layer caching significantly outperforms layer dropout, maintaining pixel-wise consistency with the original pipeline. Conversely, when the layers to be dropped are selected by our algorithm, the model can still generate images with correct semantics. However, randomly dropping layers severely compromises the model’s ability to produce acceptable images. Table 7 demonstrates that even a small proportion of layer dropout (around 10%) results in a substantial performance degradation.

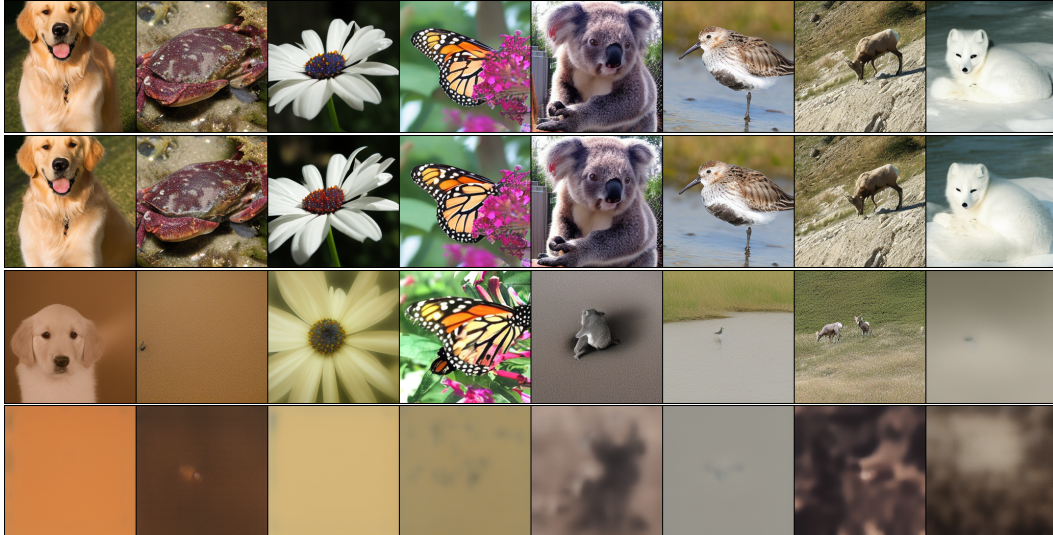


Figure 7: The quantitative results for layer dropping and layer caching in Section 4.3. (a) DDIM Pipeline with 20 NFE. (2) Our method L2C with 20 NFE (3) Learn to drop the layers by our algorithm. (4) Randomly drop layers. The results here, except the first line as the baseline, all speed up the inference by around $1.18\times\text{--}1.19\times$.

B.3 Effect of the hyper-parameter λ and θ

We find in our experiments that the router we learned is not sensitive to the hyper-parameters, including the learning rate, the training epoch, and the hyperparameters in the optimizer. The only

Table 7: Comparison with Layer Dropout

Methods	Remove Ratio	Latency(s)	Speedup	IS↑	FID↓	sFID↓	Precision↑	Recall↑
Random Drop	60/560	2.718	1.06×	9.66	112.93	153.48	10.56	65.57
Random Drop	170/560	2.439	1.18×	3.36	277.42	171.83	1.23	0.24
Learning-to-Drop	179/560	2.421	1.19×	113.93	17.35	28.46	60.25	52.68
Learning-to-Cache	176/560	2.438	1.18×	226.13	3.47	4.58	79.19	56.47

Table 8: λ and θ for training the router

Model	DiT-XL/2	DiT-XL/2	DiT-XL/2	DiT-XL/2	DiT-L/2	DiT-L/2	U-ViT-H/2	U-ViT-H/2
NFE	50	20	10	50	50	20	50	20
Resolution	256	256	256	512	256	256	256	256
Sampler	DDIM	DDIM	DDIM	DDIM	DDIM	DDIM	DPM-Solver-2	DPM-Solver-2
λ for train	1e-6	5e-6	1e-6	5e-6	1e-6	5e-6	0.1	0.1
θ for inference	0.1	0.1	0.1	0.9	0.1	0.1	0.9	0.9
Training Cost (Hour)	7.2	5.0	2.5	8.1	7.0	1.5	5.7	3.0

Table 9: Performance with different λ . Threshold θ is set to 0.1.

λ	Remove Ratio	Latency(s)	Speedup	IS↑	FID↓	sFID↓	Precision↑	Recall↑
0	0/560	2.87	1.00×	223.49	3.48	4.89	78.76	57.07
5e-7	129/560	2.55	1.13 ×	222.15	3.49	4.79	78.47	57.36
1e-6	176/560	2.45	1.17 ×	226.13	3.47	4.58	79.19	56.47
5e-6	248/560	2.28	1.26 ×	226.95	3.45	4.64	79.20	55.82
1e-5	300/560	2.15	1.33 ×	223.41	3.70	4.91	78.88	56.36
5e-5	404/560	1.92	1.49 ×	200.60	5.43	6.55	75.06	57.54
1e-4	460/560	1.79	1.60 ×	193.75	6.51	7.71	73.55	56.55

one that would affect is the λ for training and the threshold θ for inference. We list in Table 8 the λ we use that could reproduce the results in Table 1. Here the difference between DiT and U-ViT for λ comes from the difference in implementation.

The results of using different λ values are presented in Table 9. Note that λ serves as the regularization strength to control the sparsity of the router, and thus there would not exist an optimal λ for all settings. It functions as a trade-off between latency and quality, balancing the speed of inference with the fidelity of the generated images.

C Social Impact

The acceleration of diffusion transformers provides several positive social impacts, such as reducing the latency and resources required for deploying diffusion models. This enhancement improves the real-time applicability of diffusion transformers and promotes environmental sustainability. By making diffusion models more efficient, our method reduces the computational power needed for both training and inference, leading to lower energy consumption and a reduced carbon footprint. However, it is important to note that our method does not address privacy concerns, nor does it mitigate issues related to bias and fairness in diffusion models. These challenges remain when applying our method.

NeurIPS Paper Checklist

1. Claims

Question: Do the main claims made in the abstract and introduction accurately reflect the paper's contributions and scope?

Answer: [Yes]

Justification: The abstract and introduction clearly state the claims made.

Guidelines:

- The answer NA means that the abstract and introduction do not include the claims made in the paper.
- The abstract and/or introduction should clearly state the claims made, including the contributions made in the paper and important assumptions and limitations. A No or NA answer to this question will not be perceived well by the reviewers.
- The claims made should match theoretical and experimental results, and reflect how much the results can be expected to generalize to other settings.
- It is fine to include aspirational goals as motivation as long as it is clear that these goals are not attained by the paper.

2. Limitations

Question: Does the paper discuss the limitations of the work performed by the authors?

Answer: [Yes]

Justification: Section 5 discuss the limitation.

Guidelines:

- The answer NA means that the paper has no limitation while the answer No means that the paper has limitations, but those are not discussed in the paper.
- The authors are encouraged to create a separate "Limitations" section in their paper.
- The paper should point out any strong assumptions and how robust the results are to violations of these assumptions (e.g., independence assumptions, noiseless settings, model well-specification, asymptotic approximations only holding locally). The authors should reflect on how these assumptions might be violated in practice and what the implications would be.
- The authors should reflect on the scope of the claims made, e.g., if the approach was only tested on a few datasets or with a few runs. In general, empirical results often depend on implicit assumptions, which should be articulated.
- The authors should reflect on the factors that influence the performance of the approach. For example, a facial recognition algorithm may perform poorly when image resolution is low or images are taken in low lighting. Or a speech-to-text system might not be used reliably to provide closed captions for online lectures because it fails to handle technical jargon.
- The authors should discuss the computational efficiency of the proposed algorithms and how they scale with dataset size.
- If applicable, the authors should discuss possible limitations of their approach to address problems of privacy and fairness.
- While the authors might fear that complete honesty about limitations might be used by reviewers as grounds for rejection, a worse outcome might be that reviewers discover limitations that aren't acknowledged in the paper. The authors should use their best judgment and recognize that individual actions in favor of transparency play an important role in developing norms that preserve the integrity of the community. Reviewers will be specifically instructed to not penalize honesty concerning limitations.

3. Theory Assumptions and Proofs

Question: For each theoretical result, does the paper provide the full set of assumptions and a complete (and correct) proof?

Answer: [Yes]

Justification: In Appendix A

Guidelines:

- The answer NA means that the paper does not include theoretical results.
- All the theorems, formulas, and proofs in the paper should be numbered and cross-referenced.
- All assumptions should be clearly stated or referenced in the statement of any theorems.
- The proofs can either appear in the main paper or the supplemental material, but if they appear in the supplemental material, the authors are encouraged to provide a short proof sketch to provide intuition.
- Inversely, any informal proof provided in the core of the paper should be complemented by formal proofs provided in appendix or supplemental material.
- Theorems and Lemmas that the proof relies upon should be properly referenced.

4. Experimental Result Reproducibility

Question: Does the paper fully disclose all the information needed to reproduce the main experimental results of the paper to the extent that it affects the main claims and/or conclusions of the paper (regardless of whether the code and data are provided or not)?

Answer: [Yes]

Justification: In Section 4.1

Guidelines:

- The answer NA means that the paper does not include experiments.
- If the paper includes experiments, a No answer to this question will not be perceived well by the reviewers: Making the paper reproducible is important, regardless of whether the code and data are provided or not.
- If the contribution is a dataset and/or model, the authors should describe the steps taken to make their results reproducible or verifiable.
- Depending on the contribution, reproducibility can be accomplished in various ways. For example, if the contribution is a novel architecture, describing the architecture fully might suffice, or if the contribution is a specific model and empirical evaluation, it may be necessary to either make it possible for others to replicate the model with the same dataset, or provide access to the model. In general, releasing code and data is often one good way to accomplish this, but reproducibility can also be provided via detailed instructions for how to replicate the results, access to a hosted model (e.g., in the case of a large language model), releasing of a model checkpoint, or other means that are appropriate to the research performed.
- While NeurIPS does not require releasing code, the conference does require all submissions to provide some reasonable avenue for reproducibility, which may depend on the nature of the contribution. For example
 - (a) If the contribution is primarily a new algorithm, the paper should make it clear how to reproduce that algorithm.
 - (b) If the contribution is primarily a new model architecture, the paper should describe the architecture clearly and fully.
 - (c) If the contribution is a new model (e.g., a large language model), then there should either be a way to access this model for reproducing the results or a way to reproduce the model (e.g., with an open-source dataset or instructions for how to construct the dataset).
 - (d) We recognize that reproducibility may be tricky in some cases, in which case authors are welcome to describe the particular way they provide for reproducibility. In the case of closed-source models, it may be that access to the model is limited in some way (e.g., to registered users), but it should be possible for other researchers to have some path to reproducing or verifying the results.

5. Open access to data and code

Question: Does the paper provide open access to the data and code, with sufficient instructions to faithfully reproduce the main experimental results, as described in supplemental material?

Answer: [Yes]

Justification: We would release the code and the code is submitted in the supplemental material

Guidelines:

- The answer NA means that paper does not include experiments requiring code.
- Please see the NeurIPS code and data submission guidelines (<https://nips.cc/public/guides/CodeSubmissionPolicy>) for more details.
- While we encourage the release of code and data, we understand that this might not be possible, so “No” is an acceptable answer. Papers cannot be rejected simply for not including code, unless this is central to the contribution (e.g., for a new open-source benchmark).
- The instructions should contain the exact command and environment needed to run to reproduce the results. See the NeurIPS code and data submission guidelines (<https://nips.cc/public/guides/CodeSubmissionPolicy>) for more details.
- The authors should provide instructions on data access and preparation, including how to access the raw data, preprocessed data, intermediate data, and generated data, etc.
- The authors should provide scripts to reproduce all experimental results for the new proposed method and baselines. If only a subset of experiments are reproducible, they should state which ones are omitted from the script and why.
- At submission time, to preserve anonymity, the authors should release anonymized versions (if applicable).
- Providing as much information as possible in supplemental material (appended to the paper) is recommended, but including URLs to data and code is permitted.

6. Experimental Setting/Details

Question: Does the paper specify all the training and test details (e.g., data splits, hyperparameters, how they were chosen, type of optimizer, etc.) necessary to understand the results?

Answer: [Yes]

Justification: In Section 4.1 and Appendix

Guidelines:

- The answer NA means that the paper does not include experiments.
- The experimental setting should be presented in the core of the paper to a level of detail that is necessary to appreciate the results and make sense of them.
- The full details can be provided either with the code, in appendix, or as supplemental material.

7. Experiment Statistical Significance

Question: Does the paper report error bars suitably and correctly defined or other appropriate information about the statistical significance of the experiments?

Answer: [No]

Justification: We don't report error bars.

Guidelines:

- The answer NA means that the paper does not include experiments.
- The authors should answer "Yes" if the results are accompanied by error bars, confidence intervals, or statistical significance tests, at least for the experiments that support the main claims of the paper.
- The factors of variability that the error bars are capturing should be clearly stated (for example, train/test split, initialization, random drawing of some parameter, or overall run with given experimental conditions).
- The method for calculating the error bars should be explained (closed form formula, call to a library function, bootstrap, etc.)
- The assumptions made should be given (e.g., Normally distributed errors).

- It should be clear whether the error bar is the standard deviation or the standard error of the mean.
- It is OK to report 1-sigma error bars, but one should state it. The authors should preferably report a 2-sigma error bar than state that they have a 96% CI, if the hypothesis of Normality of errors is not verified.
- For asymmetric distributions, the authors should be careful not to show in tables or figures symmetric error bars that would yield results that are out of range (e.g. negative error rates).
- If error bars are reported in tables or plots, The authors should explain in the text how they were calculated and reference the corresponding figures or tables in the text.

8. Experiments Compute Resources

Question: For each experiment, does the paper provide sufficient information on the computer resources (type of compute workers, memory, time of execution) needed to reproduce the experiments?

Answer: [Yes]

Justification: In Section 4.1 Implementations

Guidelines:

- The answer NA means that the paper does not include experiments.
- The paper should indicate the type of compute workers CPU or GPU, internal cluster, or cloud provider, including relevant memory and storage.
- The paper should provide the amount of compute required for each of the individual experimental runs as well as estimate the total compute.
- The paper should disclose whether the full research project required more compute than the experiments reported in the paper (e.g., preliminary or failed experiments that didn't make it into the paper).

9. Code Of Ethics

Question: Does the research conducted in the paper conform, in every respect, with the NeurIPS Code of Ethics <https://neurips.cc/public/EthicsGuidelines>?

Answer: [Yes]

Justification: Our research conform to the NeurIPS Code of Ethics

Guidelines:

- The answer NA means that the authors have not reviewed the NeurIPS Code of Ethics.
- If the authors answer No, they should explain the special circumstances that require a deviation from the Code of Ethics.
- The authors should make sure to preserve anonymity (e.g., if there is a special consideration due to laws or regulations in their jurisdiction).

10. Broader Impacts

Question: Does the paper discuss both potential positive societal impacts and negative societal impacts of the work performed?

Answer: [Yes]

Justification: We discuss it in Appendix C

Guidelines:

- The answer NA means that there is no societal impact of the work performed.
- If the authors answer NA or No, they should explain why their work has no societal impact or why the paper does not address societal impact.
- Examples of negative societal impacts include potential malicious or unintended uses (e.g., disinformation, generating fake profiles, surveillance), fairness considerations (e.g., deployment of technologies that could make decisions that unfairly impact specific groups), privacy considerations, and security considerations.

- The conference expects that many papers will be foundational research and not tied to particular applications, let alone deployments. However, if there is a direct path to any negative applications, the authors should point it out. For example, it is legitimate to point out that an improvement in the quality of generative models could be used to generate deepfakes for disinformation. On the other hand, it is not needed to point out that a generic algorithm for optimizing neural networks could enable people to train models that generate Deepfakes faster.
- The authors should consider possible harms that could arise when the technology is being used as intended and functioning correctly, harms that could arise when the technology is being used as intended but gives incorrect results, and harms following from (intentional or unintentional) misuse of the technology.
- If there are negative societal impacts, the authors could also discuss possible mitigation strategies (e.g., gated release of models, providing defenses in addition to attacks, mechanisms for monitoring misuse, mechanisms to monitor how a system learns from feedback over time, improving the efficiency and accessibility of ML).

11. Safeguards

Question: Does the paper describe safeguards that have been put in place for responsible release of data or models that have a high risk for misuse (e.g., pretrained language models, image generators, or scraped datasets)?

Answer: [NA]

Justification: We have no new models/datasets.

Guidelines:

- The answer NA means that the paper poses no such risks.
- Released models that have a high risk for misuse or dual-use should be released with necessary safeguards to allow for controlled use of the model, for example by requiring that users adhere to usage guidelines or restrictions to access the model or implementing safety filters.
- Datasets that have been scraped from the Internet could pose safety risks. The authors should describe how they avoided releasing unsafe images.
- We recognize that providing effective safeguards is challenging, and many papers do not require this, but we encourage authors to take this into account and make a best faith effort.

12. Licenses for existing assets

Question: Are the creators or original owners of assets (e.g., code, data, models), used in the paper, properly credited and are the license and terms of use explicitly mentioned and properly respected?

Answer: [Yes]

Justification: All assets used in our paper is cited or marked in the code.

Guidelines:

- The answer NA means that the paper does not use existing assets.
- The authors should cite the original paper that produced the code package or dataset.
- The authors should state which version of the asset is used and, if possible, include a URL.
- The name of the license (e.g., CC-BY 4.0) should be included for each asset.
- For scraped data from a particular source (e.g., website), the copyright and terms of service of that source should be provided.
- If assets are released, the license, copyright information, and terms of use in the package should be provided. For popular datasets, paperswithcode.com/datasets has curated licenses for some datasets. Their licensing guide can help determine the license of a dataset.
- For existing datasets that are re-packaged, both the original license and the license of the derived asset (if it has changed) should be provided.

- If this information is not available online, the authors are encouraged to reach out to the asset's creators.

13. New Assets

Question: Are new assets introduced in the paper well documented and is the documentation provided alongside the assets?

Answer: [Yes]

Justification: Would release the code and the trained router.

Guidelines:

- The answer NA means that the paper does not release new assets.
- Researchers should communicate the details of the dataset/code/model as part of their submissions via structured templates. This includes details about training, license, limitations, etc.
- The paper should discuss whether and how consent was obtained from people whose asset is used.
- At submission time, remember to anonymize your assets (if applicable). You can either create an anonymized URL or include an anonymized zip file.

14. Crowdsourcing and Research with Human Subjects

Question: For crowdsourcing experiments and research with human subjects, does the paper include the full text of instructions given to participants and screenshots, if applicable, as well as details about compensation (if any)?

Answer: [NA]

Justification: Does not involve crowdsourcing nor research with human subjects.

Guidelines:

- The answer NA means that the paper does not involve crowdsourcing nor research with human subjects.
- Including this information in the supplemental material is fine, but if the main contribution of the paper involves human subjects, then as much detail as possible should be included in the main paper.
- According to the NeurIPS Code of Ethics, workers involved in data collection, curation, or other labor should be paid at least the minimum wage in the country of the data collector.

15. Institutional Review Board (IRB) Approvals or Equivalent for Research with Human Subjects

Question: Does the paper describe potential risks incurred by study participants, whether such risks were disclosed to the subjects, and whether Institutional Review Board (IRB) approvals (or an equivalent approval/review based on the requirements of your country or institution) were obtained?

Answer: [NA]

Justification: Does not involve crowdsourcing nor research with human subjects

Guidelines:

- The answer NA means that the paper does not involve crowdsourcing nor research with human subjects.
- Depending on the country in which research is conducted, IRB approval (or equivalent) may be required for any human subjects research. If you obtained IRB approval, you should clearly state this in the paper.
- We recognize that the procedures for this may vary significantly between institutions and locations, and we expect authors to adhere to the NeurIPS Code of Ethics and the guidelines for their institution.
- For initial submissions, do not include any information that would break anonymity (if applicable), such as the institution conducting the review.